doi:10.3772/j.issn.1006-6748.2016.02.013

Improved Roberts operator for detecting surface defects of heavy rails with superior precision and efficiency①

Shi Tian (石 甜)②*, Kong Jianyi*, Wang Xingdong*, Liu Zhao*, Xiong Jianliang**
(*School of Machinery and Automation, Wuhan University of Science and Technology, Wuhan 430081, P. R. China)
(**Wuhan Iron and Steel (Group) Corporation, Wuhan 430083, P. R. China)

Abstract

An experimental platform accompanying with the improved Roberts algorithm has been developed to achieve accurate and real-time edge detection of surface defects on heavy rails. Detection results of scratching defects show that the improved Roberts operator can attain accurate positioning to defect contour and get complete edge information. Meanwhile, a decreasing amount of interference noises as well as more precise characteristic parameters of the extracted defects can also be confirmed for the improved algorithm. Furthermore, the BP neural network adopted for defects classification with the improved Roberts operator can obtain the target training precision with 98 iterative steps and time of 2s while that of traditional Roberts operator is 118 steps and 4s. Finally, an enhanced defects identification rate of 13.33% has also been confirmed after the Roberts operator is improved. The proposed detecting platform will be positive in producing high-quality heavy rails and guaranteeing the national transportation safety.

Key words: detecting platform, Roberts operator, defects detection, heavy rails, identification rate

0 Introduction

Recent years have seen rapid development of high-speed rail network, which are putting more demand on the quality of heavy rails. Accordingly, the accurate and real-time detection of surface defects on heavy rails among their productive process can play a significant role in improving the track quality and guaranteeing the national transportation safety. Yet, numerous methods about the defects detection on surfaces of heavy rails have been developed among many walks of researchers. Oregui, et al. have detected damaged conditions in railway tracks by applying a statistical method based on the frequency response function in combination with non-destructive field hammer test measurements[1]. Mariani, et al. have developed a prototype by using an ultrasonic air-coupled guided wave signal generation and air-coupled signal for high-speed and non-contact rail defect detection[2]. Antipov, et al. have adopted a magnetic flux leakage (MFL) method by considering the limiting detection depth of the defects on the railway surface to realize nondestructive detection, which must be equipped with a costy magnetizing system[3]. Popovic, et al. have also investigated the defects of railways by using the visual inspection as well as the eddy current testing[4]. Nevertheless, the statistical and visual method for defects detection must mainly rely on the experience of technicians leading to a low detection accuracy and low productivity. Meanwhile, non-contact ultrasonic guided wave inspection of rails requires a specialized filtering approach based on an electrical impedance matching device, which adds both the costs and complexity concerns for the defects detection. Besides, the MFL method and the eddy current test are not suitable for detecting the complicated surfaces especially for the heavy rails with poor productive surroundings, which may result in false or even missing detections. Consequently, developing an accurate, facile and rapid method for detecting the surface defects of heavy rails is yet a severe challenge.

The machine vision technology, as one the most promising methods for edge detection, has gained ex-

① Supported by the National Natural Science Foundation of China (No. 51174151), Major Scientific Research Projects of Hubei Provincial Department of Education (No. 2010Z19003), Natural Science Foundation of Science and Technology Department of Hubei Province (No. 2010CDB03403), and Student Research Fund of WUST (No. 14ZRB047).

② To whom correspondence should be addressed. E-mail: Tianshiwust@163.com

Received on Oct. 9, 2015

tensive attention in various application areas due to its accurate, real-time and controllable properties[5-7]. And also the frequently adopted recognition operators consist of Roberts[8,9], Prewitt[10,11], Canny[12,13], p-Laplacian[14] and Gaussian[15] etc. Among these operators, Roberts operator can approximate the gradient amplitude by using the difference between the adjacent pixels at diagonal directions for edge detection leading to a superior edge detection performance at the horizontal and vertical direction than other operators[16], which has attained much popularity among various research fields. In Ref. [17], the Roberts algorithm was adopted to recognize the Persian font with the decreasing calculation and improved detection speed. In Ref. [18], Roberts operator was applied to help farmers to identify the degree of crop diseases in agricultural engineering, which can perform well for edge detection of agricultural crop leaf image. Ref. [19] used the Roberts operator to evaluate the effect of the gas shielded welding molten pool image edge detection. Ref. [20] analyzed the frequency features of Roberts as well as other operators to select the appropriate operator for detecting edge in medical magnetic resonance imaging edge processing. However, seldom investigations on Roberts operator have been reported about the detection of surface defects for heavy rails despite the above mentioned application fields.

Additionally, Roberts operator can just detect the gradient magnitude via the diagonal adjacent pixels without consideration of the horizontal and vertical adjacent pixels, which might negatively affect its detection effect. Meanwhile, the discontinuous and missing object contour edges can also be found for its sensitivity to noise interference. To overcome the weak points of the gradient amplitude calculation for traditional Roberts algorithm, a new method to determine the pixel gradient magnitude by calculating the first order partial derivative of a finite-difference gradient amplitude with the adding vertical and horizontal adjacent pixels is proposed in this work. This method takes into account the accurate positioning for edge gradient magnitude calculation as well as the noise suppression requirements, which can make the edge detection more accurate. Meanwhile, an experimental platform for detecting the surface defects of heavy rails has also been set up to evaluate the detection effect with the improved Roberts operator.

1 Edge detection algorithm

Edge detection algorithm with typical Roberts operator can approximately calculate the gradient amplitude by applying the difference between adjacent pixels at the diagonal directions. Meanwhile, the finite difference between a pair of vertical directions can be regarded as an approximate solution of the gradient when processing the image pixels[21]. Therefore, its gradient magnitude M_0 can be firstly calculated by the finite-difference method. Then, the approximate continuous gradient amplitude value $M_0(m, n)$ of the Roberts operator at the finite difference point $(m+1/2, n+1/2)$ can be obtained by differential calculation. Meanwhile, $M_0(m, n)$ can be compared with the setting gray threshold G_0 to distinguish the pixel point (m, n). If $M_0(m, n) > G_0$, the pixel point (m, n) can be judged as the edge point. Otherwise, it is not the edge point.

However, the edge detection with the Roberts operator only considers 4 pieces of pixel information at the diagonal direction while ignoring the horizontal and vertical pixels. The algorithm is unable to detect the local edge of the gray value with slow change among the horizontal or vertical adjacent pixels. Moreover, the Roberts operator cannot effectively suppress the noise for its sensitivity to noise interference, which might count for the discontinuous and missing object contour edges of the defects images on heavy rails.

Based on the pixel information at the diagonal direction, this work develops an improved Roberts operator by adding the horizontal and vertical pixels information within 8 pixels neighborhood. Then the proposed Roberts operator can calculate the pixel gradient magnitude by the first order partial derivative of a finite-difference gradient amplitude with all the adjacent pixels. The adding pixels information will make the detecting edge information more comprehensive and the detecting precision more accurate. The finite-difference with directions of 0°, 45°, 90° and 135° can be respectively described as $f_0(x, y)$, $f_{45}(x, y)$, $f_{90}(x, y)$ and $f_{135}(x, y)$ as follows:

$$f_0(x, y) = t(x-1, y) - t(x+1, y) \quad (1)$$

$$f_{45}(x, y) = t(x+1, y-1) - t(x-1, y+1) \quad (2)$$

$$f_{90}(x, y) = t(x, y-1) - t(x, y+1) \quad (3)$$

$$f_{135}(x, y) = t(x-1, y-1) - t(x+1, y+1) \quad (4)$$

The corresponding convolution operators f_0, f_{45}, f_{90}, f_{135} can be described in sequence as follows:

$$\begin{bmatrix} 0 & 0 & 0 \\ 1 & 0 & -1 \\ 0 & 0 & 0 \end{bmatrix} \begin{bmatrix} 0 & 0 & 1 \\ 0 & 0 & 0 \\ -1 & 0 & 0 \end{bmatrix} \begin{bmatrix} 0 & 1 & 0 \\ 0 & 0 & 0 \\ 0 & -1 & 0 \end{bmatrix} \begin{bmatrix} 1 & 0 & 0 \\ 0 & 0 & 0 \\ 0 & 0 & -1 \end{bmatrix}$$

Finally, the approximate gradient amplitude M_1 of the improved Roberts algorithm can be described by

Eq. (5). By comparing M_1 and G_0, the edge point can be judged.

$$M_1 = |f_0(x, y)| + |f_{45}(x, y)| + |f_{90}(x, y)| + |f_{135}(x, y)| \quad (5)$$

2 Experimental platform

The experimental platform for detecting surface defects of heavy rails is shown in Fig. 1, which comprises of the parallel computer system, bracket structures, imaging system, LED light sources and cable system etc. The image-forming system with CCD cameras, filters and lens is fixed on the portal frame, which can slip along the sliding rail of the platform. The rail surface images extracted from the imaging system can be transmitted to the parallel computer system. After the image signals being processed and analyzed, the defects recognition of the heavy rails will be achieved. Meanwhile, the detection effect of the improved Roberts operator can also be evaluated by considering the integrity of edge information as well as the detection time. Fig. 2 exhibits the scratching defect image from the heavy rails extracted by using the designed detecting experimental platform.

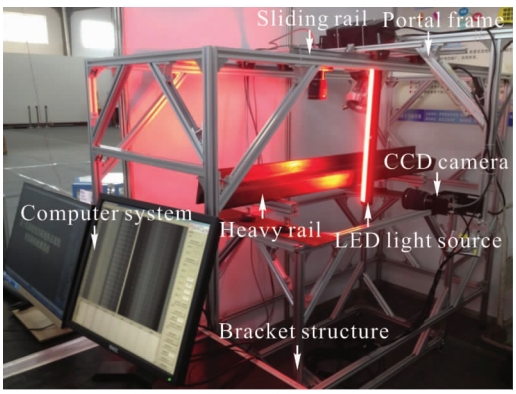

Fig. 1 The experimental platform for detecting the surface defects of heavy rails

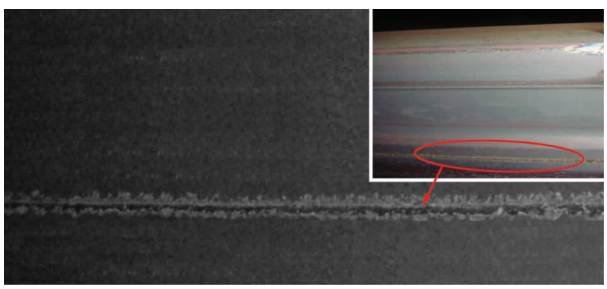

Fig. 2 The extracted scratching defect image from the heavy rails

Extracting an eligible defect image by the experimental platform is the precondition for the defect detection and recognition. Hereon, the image signals to noise rate (*ISNR*) have been applied to evaluate the quality of the extracting defect images, which can be calculated by[22]

$$ISNR = \frac{D_{max} - D_{min}}{B_{max} - B_{min}} \quad (6)$$

where D_{max} and D_{min} are corresponding to the maximum and minimum gray values of the defect images, respectively. B_{max} and B_{min} respectively refer to the maximum and minimum gray values in the background region outside the scratching area. And also Ref. [23] reported that a qualified defect image can be obtained when $ISNR > 1.8$. The grey histogram of the extracted defect images, as a statistical frequency to characterize every appearance of grey value, is shown in Fig. 3. Obviously, D_{max} and D_{min} can be respectively seen with 169 and 13 in the statistical histogram. Meanwhile, the grey scattergram in the background area measured for five times at different positions of the extracted image is depicted in Fig. 4, among which B_{max} and B_{min} respectively with 92.6 and 18.2 can be attained after the average process of the five measurements of the background grey. Then the image signal to noise rate can be calculated by $ISNR = (169 - 13)/(92.6 - 18.2) = 2.1$, which is larger than 1.8 suggesting a qualified scratching image extracted via the designed detecting experimental platform.

3 Results and discussion

3.1 Edge detection effect

Influenced by the instability of the rails production environment as well as the light sources, uneven illumination may be found with the collected scratching

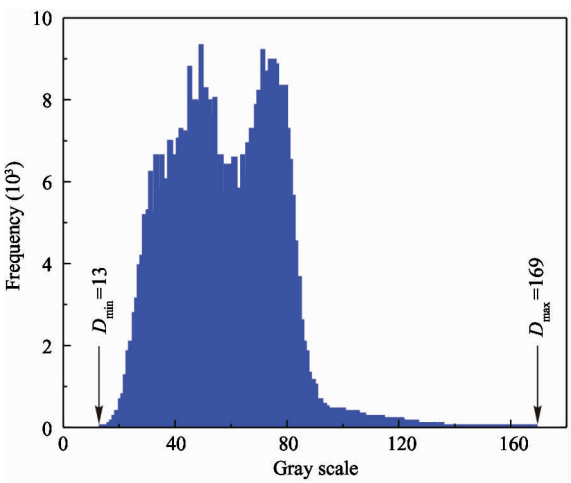

Fig. 3 The statistical gray histogram characterizing frequency of every appearance of grey value on extracted defect image

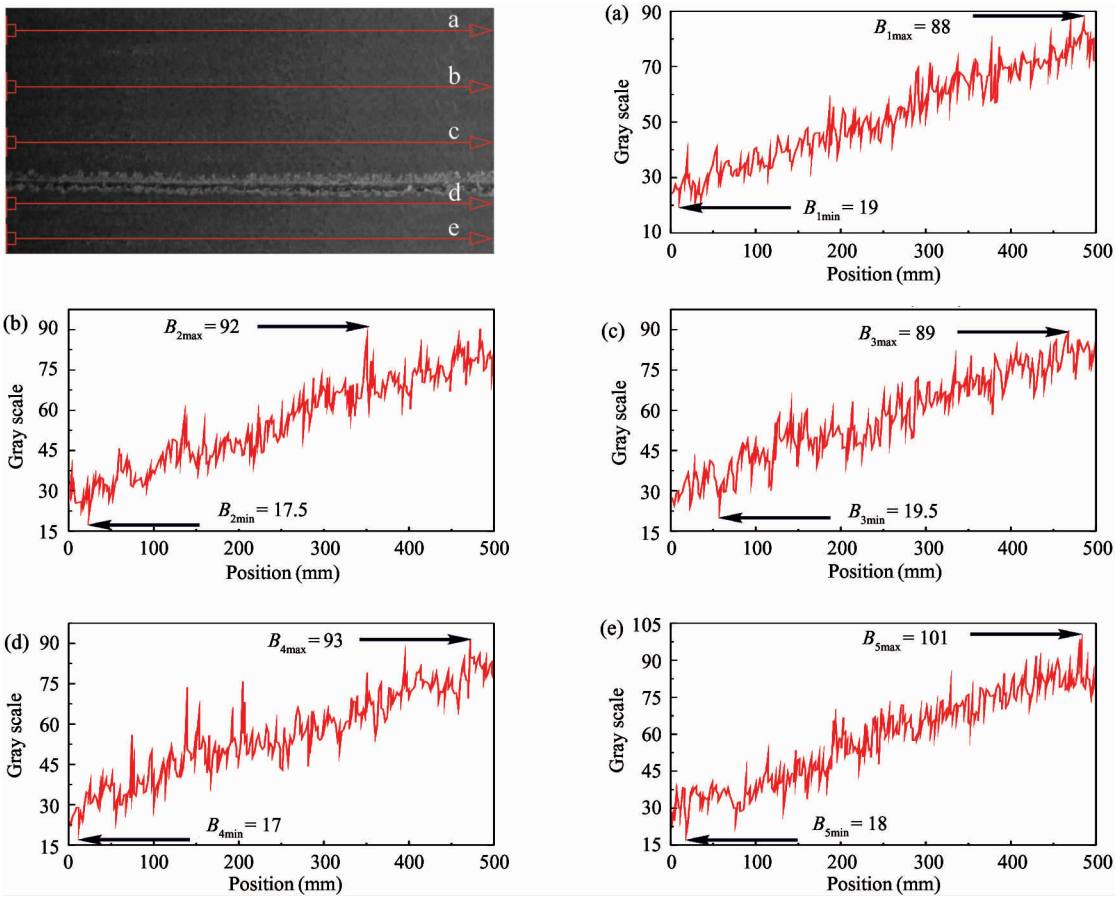

Fig. 4 The gray scattergram in background area measured for five times at different positions of the extracted defect image

images, which will exert a negative effect on the coming edge detection and eigenvalue extraction. Herein, as shown in Fig. 5(a), the imsubtract function of Matlab has been adopted to weaken the background interference to the scratching defect, which can also reduce the effect of asymmetrical illumination on the defect image. After the background interference is removed, the edge detection images of the extracted scratching defects with Roberts operator and improved Roberts operator are respectively exhibited in Fig. 5(b) and Fig. 5(c). Obviously, the scratching defect edge image obtained by the improved Roberts operator is more holonomic and continuous than the edge image extracted by Roberts operator. And also the extracted edge information obtained via the improved Roberts operator can be commendably coincide with the shape characteristics of the scratching defect. Besides, a decreasing amount of noise points on edge image can also be seen clearly with the improved Roberts operator demonstrating an excellent noise suppression capacity. As it is well known, the improved Roberts operator can easily achieve a precise position of the defect and also extract more accurate characteristic parameters after

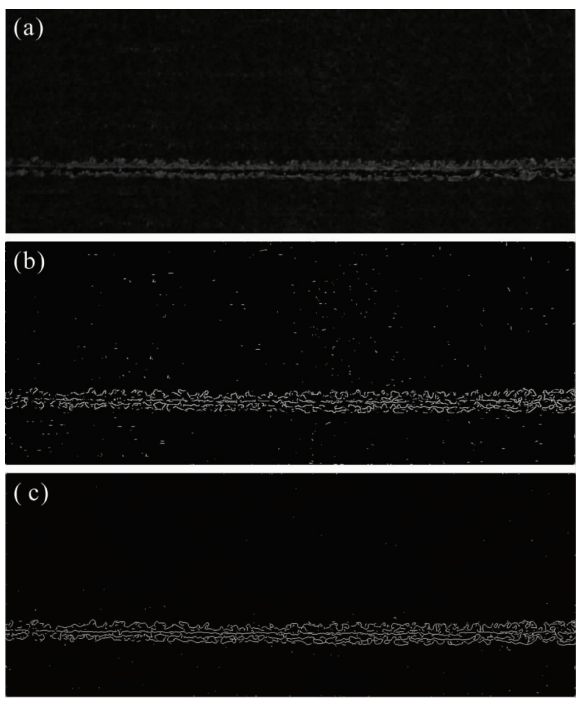

(a) corresponding to the scratching defect image after removing the background interference. (b) and (c) respectively depicting the edge detection images with Roberts operator and improved Roberts operator

Fig. 5 Edge detection comparison of the extracting scratching defects

being added with the horizontal and vertical pixels information, which can account for its integrated edge detection as well as the superior ability of noise suppression.

The extracted characteristic parameters of the scratching defects are important foundation of the identification and classification of defects. A high recognition rate of the defect can be got from its accurate characteristic parameters. After the binarization process of the scratching defect images, the extracted 24 characteristic parameters can be attained. And the extracted parameters of the defect images with the improved Roberts operator and Roberts operator are exhibited in Table 1 and Table 2, respectively.

Table 1 Extracted characteristic parameters of the defect image by using improved Roberts operator

Characteristic	Value	Characteristic	Value	Characteristic	Value	Characteristic	Value
Dispersity	4522	Gray entropy	7.3	Background energy	0.39	Second moment invariants	12.47
Rectangle degree	0.36	Average background gray	57	Background homogeneity	0.99	Third moment invariants	24.81
Aspect ratio	0.05	Background gray codomain	155	Relevance	0.94	Fourth moment invariants	24.64
Average gray	68	Background gray variance	17.4	Energy	0.42	Fifth moment invariants	49.4
Gray codomain	140	Background gray entropy	5.8	Homogeneity	0.99	Sixth moment invariants	29.1
Gray variance	23.6	Background correlation	0.96	First moment invariants	5.96	Seventh moment invariants	50.15

Table 2 Extracted characteristic parameters of the defect image by using Roberts operator

Characteristic	Value	Characteristic	Value	Characteristic	Value	Characteristic	Value
Dispersity	5232	Gray entropy	7	Background energy	0.45	Second moment invariants	12.47
Rectangle degree	0.39	Average background gray	59	Background homogeneity	0.98	Third moment invariants	24.82
Aspect ratio	0.05	Background gray codomain	159	Relevance	0.92	Fourth moment invariants	24.64
Average gray	70	Background gray variance	18	Energy	0.45	Fifth moment invariants	49.44
Gray codomain	144	Background gray entropy	6	Homogeneity	0.98	Sixth moment invariants	30.9
Gray variance	24	Background correlation	0.95	First moment invariants	5.99	Seventh moment invariants	50.19

3.2 Neural network classification

To realize rapid and accurate classification of the extracted defects on heavy rails, a BP neural network with the ability of self-learning and self-organization has been applied for defects identification and classification. As shown in Fig. 6, the BP neural network is designed with 24 characteristic parameters in the input layer, 4 identification parameters in an output layer and also two hidden layers respectively with 15 and 4 neurons.

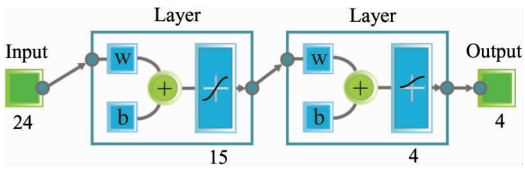

Fig. 6 BP neural network image with 24 characteristic parameters in the input layer, 4 identification parameters in an output layer and also two hidden layers respectively with 15 and 4 neurons

30 sets of the scratching defects images are obtained by the detecting experimental platform. After the pretreatment, edge detection and characteristic parameters extraction of the defect images, 15 groups of characteristics can be elected as the training specimens and the others as the testing specimens. Meanwhile,

the BP neural network is simulated by Matlab, among which the minimum mean square error is set as 0.01, the maximum training frequency as 500 and the learning step as 0.15. When the mean square error falls below 0.01 or the training step reach to 500, the iterative will closure and the system will be convergent immediately. Fig. 7(a) exhibits the BP neural network training curve for defects edge detection with the inputting characteristic parameters extracted by using Roberts operator. Clearly, the mean square error can reach to the optimal training precision of 0.00903 with 118 steps. For the improved Roberts operator in Fig. 7(b), however, the mean square error can get the target precision less than 0.01 only with 98 steps. In addition, the training results through the improved Roberts operator can achieve the target precision with 2 s, which is less than Roberts operator for 4 s. Based on the above analysis, the improved Roberts operator can achieve the training accuracy with fewer steps and time for its more accurate characteristic parameters, which can significantly improve the identification efficiency of the scratching defects on heavy rails.

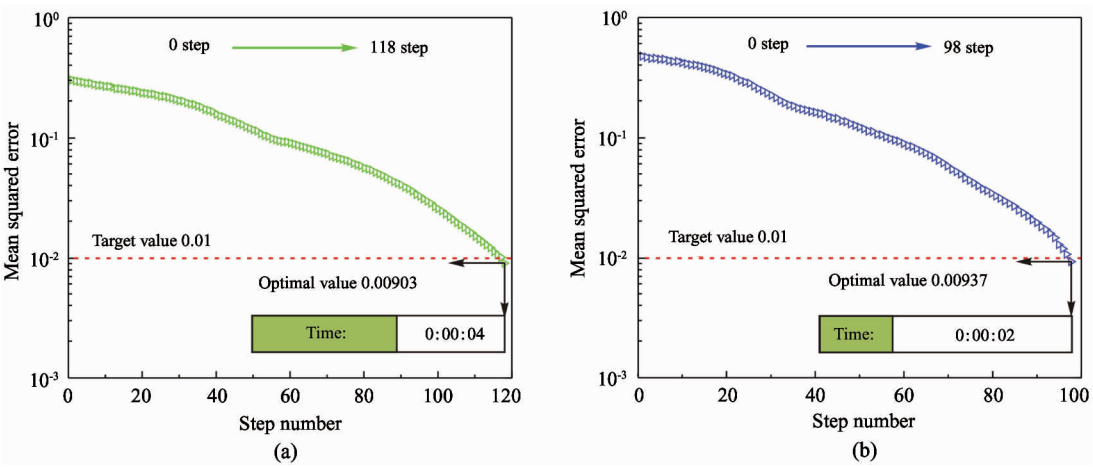

(a) and (b) referring to the BP neural network training curve for defects edge detection with the inputting characteristic parameters extraced by using Roberts operator and improved Roberts operator, respectively

Fig. 7 Defect edge detection results comparison

3.3 Recognition accuracy analysis

The outputting data of the tested specimens with the inputting characteristics parameters of Roberts operator and the improved Roberts operator after being processed with BP neural network is listed in Table 3. The outputting value will be regarded as 1 if it is greater than 0.5. Otherwise, it will be ascertained as 0. The discriminant result with 4 parameters of (0, 1, 0, 0) can be identified as the target defect. Clearly, the correct distinguishing specimens based on the Roberts operator and the improved Roberts operator are 12 and 14, respectively. Accordingly, the improved Roberts operator has got an elevated defect identification rate of 13.33% than the Roberts operator. Based on the above analysis, the proposed improved Roberts operator with the adding horizontal and vertical pixels information can detect the surface defects on heavy rails with higher identification rate as well as higher efficiency and accuracy.

4 Conclusion

An experimental platform with improved Roberts operator has been constructed to detect the surface defects of heavy rails. After the edge detection of the extracted defect images, the accurate image positioning, complete edge information and superior noise suppression capacity can be attained for the adding pixels information. Meanwhile, the target training precision with less convergent steps and time can also be obtained owing to the extracting precise characteristic parameters of the defects. Besides, an improved defect identification rate of 13.33% can be finally confirmed for the improved Roberts operator.

Table 3 The output data of the tested specimens with the inputting characteristics parameters of Roberts operator and the improved Roberts operator after BP neural network process

Sample	Output value (Roberts operator)	Discriminant result	Output value (improved Roberts operator)	Discriminant result
1	(0.0693, 0.9508, 0.0238, 0.0028)	(0, 1, 0, 0)	(0.0207, 0.9205, 0.0364, 0.0318)	(0, 1, 0, 0)
2	(0.1777, 0.9366, 0.0287, 0.0041)	(0, 1, 0, 0)	(0.0311, 0.9924, 0.0614, 0.1853)	(0, 1, 0, 0)
3	(0.9403, 0.0077, 0.0448, 0.0066)	(1, 0, 0, 0)	(0.0177, 0.9181, 0.0984, 0.0373)	(0, 1, 0, 0)
4	(0.0883, 0.9058, 0.0241, 0.0217)	(0, 1, 0, 0)	(0.0182, 0.9005, 0.0209, 0.0412)	(0, 1, 0, 0)
5	(0.0063, 0.9958, 0.1332, 0.0366)	(0, 1, 0, 0)	(0.0182, 0.9015, 0.0229, 0.0412)	(0, 1, 0, 0)
6	(0.0101, 0.8936, 0.0171, 0.0077)	(0, 1, 0, 0)	(0.0231, 0.9104, 0.0864, 0.0247)	(0, 1, 0, 0)
7	(0.0729, 0.9444, 0.0315, 0.0153)	(0, 1, 0, 0)	(0.9821, 0.0344, 0.1548, 0.1306)	(1, 0, 0, 0)
8	(0.1483, 0.9785, 0.0263, 0.0138)	(0, 1, 0, 0)	(0.0278, 0.9588, 0.1503, 0.1418)	(0, 1, 0, 0)
9	(0.9624, 0.0852, 0.0172, 0.0033)	(1, 0, 0, 0)	(0.0335, 0.9721, 0.0498, 0.1523)	(0, 1, 0, 0)
10	(0.1966, 0.9645, 0.0259, 0.0046)	(0, 1, 0, 0)	(0.0307, 0.9161, 0.3316, 0.0762)	(0, 1, 0, 0)
11	(0.1891, 0.9985, 0.0088, 0.0549)	(0, 1, 0, 0)	(0.0254, 0.9933, 0.0425, 0.1507)	(0, 1, 0, 0)
12	(0.0003, 0.9479, 0.0287, 0.0125)	(0, 1, 0, 0)	(0.1369, 0.8928, 0.0867, 0.0009)	(0, 1, 0, 0)
13	(0.0148, 0.9009, 0.0291, 0.0165)	(0, 1, 0, 0)	(0.0712, 0.9307, 0.0606, 0.0455)	(0, 1, 0, 0)
14	(0.9727, 0.0788, 0.0308, 0.0895)	(1, 0, 0, 0)	(0.0382, 0.8728, 0.1961, 0.0157)	(0, 1, 0, 0)
15	(0.0148, 0.9967, 0.0036, 0.0508)	(0, 1, 0, 0)	(0.0981, 0.9701, 0.1219, 0.0038)	(0, 1, 0, 0)

References

[1] Oregui M, Li Z, Dollevoet R. Identification of characteristic frequencies of damaged railway tracks using field hammer test measurements. *Mechanical Systems and Signal Processing*, 2015, 54-55: 224-242

[2] Mariani S, Nguyen T V, Zhu X, et al. Non-contact ultrasonic guided wave inspection of rails: field test results and updates. In: Proceedings of the Conference on Sensors and Smart Structures Technologies for Civil, Mechanical, and Aerospace Systems, San Diego, USA, 2015. 94351(5): V011T06A012

[3] Antipov A G, Markov A A. Evaluation of transverse cracks detection depth in MFL rail NDT. *Russian Journal of Nondestructive Testing*, 2014, 50(8): 481-490

[4] Popovic Z, Brajovic L, Lazarevic L, et al. Rail defects head checking on the serbian railways. *Tehnicki Vjesnik-Technical Gazette*, 2014, 21(1): 147-153

[5] Kumar B M, Ratnam M M. Machine vision method for non-contact measurement of surface roughness of a rotating workpiece. *Sensor Review*, 2015, 35(1): 10-19

[6] Balasundaram M K, Ratnam M M. In-process measurement of surface roughness using machine vision with subpixel edge detection in finish turning. *International Journal of Precision Engineering and Manufacturing*, 2014, 15(11): 2239-2249

[7] Hong K, Chalup S K, King R A R. Affective visual perception using machine pareidolia of facial expressions. *IEEE Transactions on Affective Computing*, 2014, 5(4): 352-363

[8] Abreu E M C, Mendes A C R, Oliveira W, et al. The noncommutative doplicher-fredenhagen-roberts-amorim space. *Symmetry Integrability and Geometry-Methods and Applications*, 2010, 6: 1-37

[9] Cotaescu I I. The Schrodinger picture of the dirac quantum mechanics on spatially flat roberts on-walker backgrounds. *Modern Physics Letters A*, 2007, 22(39): 2965-2969

[10] Zhang H, Zhu Q P, Fan C E, et al. Image quality assessment based on Prewitt magnitude. *AEU-International Journal of Electronics and Communications*, 2013, 67(9): 799-803

[11] Shang J Y, Zhang Y, Zhang Q B, et al. Distorted target recognition based on Prewitt operator combined with MACH filter. In: Proceedings of the 3rd Asia Pacific Conference on Optics Manufacture, Changchun, China, 2013. 523-528

[12] Panetta K A, Agaian S S, Nercessian S C, et al. Shape-dependent canny edge detector. *Optical Engineering*, 2011, 50(8): 087008-087012

[13] Zheng Y F, Zhou Y L, Zhou H, et al. Ultrasound image edge detection based on a novel multiplicative gradient and Canny operator. *Ultrasonic Imaging*, 2015, 37(3): 238-250

[14] Cetin E, Topal F S. Existence of solutions for fractional four point boundary value problems with p-Laplacian operator. *Journal of Computational Analysis and Applications*, 2015, 19(5): 892-903

[15] Scotney B W, Coleman S A. Improving angular error via systematically designed near-circular Gaussian-based feature extraction operators. *Pattern Recognition*, 2007, 40(5): 1451-1465

[16] Singh H, Kaur T. Empirical study of various edge detection techniques for gray scale images. *International Journal of Advanced Research in Computer Science and Software Engineering*, 2013, 3(8): 76-80

[17] Khosravi H, Kabir E. Farsi font recognition based on So-

bel-Roberts features. *Pattern Recognition Letters*, 2010, 31(1): 75-82

[18] Wang B L, Cao Y, Xiao H M, et al. The edge extraction of agricultural crop leaf. In: Proceedings of the Conference on Piageng-Image Processing and Photonics for Agricultural Engineering, Zhangjiajie, China, 2009. 748916-748917

[19] Liu X G, Zhao B. Based on the CO_2 gas shielded welding molten pool image edge detection algorithm. In: Proceedings of the 2nd International Conference on Industrial Design and Mechanics Power, Nanjing, China, 2013. 840-844

[20] Wu J, Ding H, Wang G, et al. The frequency features and application of edge detection differential operators in medical image. *Journal of biomedical engineering*, 2005, 22 (1): 82-85

[21] Zhang J Y. Edge detection in glass fragmentation images based on one order differential operator. In: Proceedings of the 2nd International Conference on Computer Engineering and Applications, Bali Island, Indonesia, 2010, 591-594

[22] Wang W Y. Selecting the optimal gaussian filtering scale via the SNR of image. *Journal of Electronics & Information Technology*, 2009, 31(10): 2483-2487 (In Chinese)

[23] Liu Y J. Research on imaging optimization and depth information extraction of steel plate surface defects based on image processing: [Ph. D dissertation]. Wuhan: Wuhan University of Science and Technology, 2011. 62-70

Shi Tian, born in 1988. She is currently pursuing the Ph. D. degree in School of Machinery and Automation, Wuhan University of Science and Technology. She received the BS degree in Wuhan University of Science and Technology in 2012. Her research interests include defects detection technology, machine vision technology, neural network technology and computer technology.